Bulgarian Chemical Communications, Volume 49 Special Issue C (pp. 194– 204) 2017

Electrochemical preparation of Ag nanoparticles involving choline chloride – glycerol deep eutectic solvents

A. Cojocaru[1,2], O. Brincoveanu[2], A. Pantazi[2], D. Balan[2], M. Enachescu[2], T. Visan[1,2], L. Anicai[2]*

[1]*Depart. Inorganic Chemistry, Physical Chemistry and Electrochemistry, POLITEHNICA University of Bucharest, Calea Grivitei 132, Bucharest, Romania*

[2]*Center of Surface Science and Nanotechnology, University POLITEHNICA of Bucharest, Splaiul Independentei 313, Bucharest, Romania*

Received November 4, 2016 Revised March 6, 2017

The paper reports studies about electrochemical synthesis of silver nanoparticles (Ag NPs) at 25^{o}C involving choline chloride – glycerol deep eutectic solvent and pulse reversed current. It was demonstrated that cyclic voltammetry proves to be useful tool to evaluate the optimum content of stabilizer polyvinylpyrrolidone through analysis of the anode current peak values against the cycle's number, as an indicator of the colloidal nano-Ag amount formed into the solution. It is shown that the Ag^{+}/Ag couple on glassy carbon electrode exhibits almost reversible behavior with diffusion control of cathodic process and a stripping anodic process. Based on Dynamic Light Scattering measurements and scanning electron micrographs it has been found out that through a proper selection of the pulse regime, the nanoparticles size may be controlled. The obtained Ag NPs showed sizes in the range of 60-200 nm, depending on the electrochemical synthesis conditions.

Key words: Ag nanoparticles, electrochemical synthesis, deep eutectic solvents, choline chloride, glycerol.

INTRODUCTION

Recently, a special attention has been paid to the synthesis of nanomaterials based on silver nanoparticles (Ag NPs) that may be applied in antimicrobial and antibacterial coatings [1-3], medicine, pharmacy and cosmetology [4-6], electronics and energy sources [7-9], or sensing [10-14], due to their respective biological, physical, chemical, electronic properties and catalytic activity, distinctly different from those of the bulk metal. It is also known that the collective oscillation of conduction electrons in Ag nanostructures results in surface plasmon resonance, enabling their extensive use in plasmonics, optical sensing, and surface-enhanced Raman scattering (SERS) detection [15,16].

The synthesis of silver nanoparticles may be carried out by different methods, but the most usual ones are chemical reduction methods involving the reduction of silver salt by a reducing agent in the presence of suitable stabilizer. Thus, silver nanoparticles can be prepared via a simple technique (i.e., the 'silver mirror reaction') [17]. However, the electrochemical deposition [18-22] used for the synthesis of Ag NPs in various aqueous or non-aqueous media is an inexpensive, effective, simple and versatile route toward shape-controlled synthesis of metal nanocrystals. The electrolysis parameters like the electrode potential or current density can be tuned continuously and reversibly. The method has however its limitations, because the deposition of silver on the cathode diminishes the current efficiency. Better control may be achieved using sonoelectrochemistry to prepare monodisperse silver NPs [23]; ultrasounds include the cleaning of electrodes and the acceleration of mass transport and reaction rates. Electrochemical deposition of Ag NPs was also successfully applied in ionic liquids as dispersing media [24-32].

In general, controlling the size, shape, and structure of metal nanoparticles during both the synthesis and the usage is technologically important because of correlation with their properties. This may be performed by using capping agents which preferentially stabilize a specific set of crystal facets and thus guide the nanocrystals to grow into different shapes with very narrow size distribution. Historically, quaternary ammonium salts were among the most common classes of stabilizing agents for metal nanoparticles [33]. Li et al. [32] have achieved the controllable electrochemical synthesis of Ag nanoparticles of diameters 2–13 nm from a quaternary ionic liquid (1-butyl-3-methyl-imidazolium chloride) microemulsion. Ahmadi et al. [5] have synthesized Ag NPs on the surface of a glassy carbon electrode modified with *p-tert*-butylcalix[4]arene and *p-tert*-butylcalix[6]arene by

To whom all correspondence should be sent:
E-mail: lanicai@itcnet.ro

the reduction of Ag^+ at an open circuit potential, followed by the electrochemical reduction of the Ag^+.

Among the other additives as capping and steric stabilizing agents preventing agglomeration, there have been reports of silver nanoparticle shape-selective synthesis using poly(N-vinyl pyrrolidone) PVP [34-37], because it manipulates the growth by selectively adhering to certain crystallographic planes. This capping agent prevents uncontrolled particle growth and agglomeration like particle clusters. PVP as capping agent surrounds the nucleated particle and naturally restricts the particle from growing. PVP is a homopolymer with a polyvinyl backbone and its repeating units contain a highly polar amide group that confers hydrophilic and polar-attracting properties. The non-polar methylene groups both in the backbone and in the ring confer hydrophobic properties [36]. The PVP content in the electrolyte had a significant influence on silver nanoparticles morphology and optical properties. Tang et al. [23] demonstrated the controllability of the distance of reaction conditions away from equilibrium over a wide range for the synthesis of silver NSs with the assistance of PVP. Not only dendritic rods, dendritic sheets, and flower-like dendrites, but also Ag NPs with spherical or oval shapes and surface structure including snow flake-like and nanothorns were prepared in this way.

In this work we present some preliminary results on the electrochemical synthesis of silver nanoparticles (Ag NPs) using choline chloride (2-hydroxy-ethyl-trimethyl ammonium chloride) - glycerol mixture as electrolyte and pulse reversed current. Recently the possibility of forming ionic liquids as an eutectic of a quaternary ammonium salt (most used being choline chloride) with amides, glycols (such as glycerol) or carboxylic acids, named 'hydrogen-bond donors' has been demonstrated [38-40]. These media are known as 'deep eutectic solvents' (DESs) being also called 'ionic liquid analogues'. DESs are used as sustainable media for the creation of well-defined nanoscale and functional materials involving shape-controlled nanoparticles. Compared to ionic liquids, DESs are cheaper, much less toxic and mostly biodegradable. Other advantages of DESs are their non-volatility, non-inflammability and good air and water stability. DESs have been regarded as the most promising environmentally benign and cost-effective alternatives to conventional ionic liquids and volatile organic solvents. Although they share many characteristics and properties with ionic liquids, they represent a different type of solvent, because in contrast to ionic liquids, which are composed of one type of discrete anion and cation, DESs are formed from a eutectic mixture of Lewis and Brønsted acids and bases. The preparation of DESs is simple, just by mixing the components and heating them up under stirring. The method is safe and cost effective because it may be carried out with 100% atom economy, without purification being required, which would favor large-scale applications of DESs.

DESs have a large depression in their freezing points compared to the pure substances. For example, the DES mixture formed from choline chloride (ChCl, m.p. = 302°C) and glycerol (m.p. = 18°C) at 1:2 molar ratio has a melting point of −40°C [41]. This ionic liquid, denoted here as ILG, trade name Glyceline, is stable and transparent at room temperature. The mixture can even be prepared from food-grade components. The physical–chemical properties of ILG are similar to properties of other DESs and of traditional ionic liquids, namely density, viscosity, electrical conductivity, potential window, and their temperature dependence. However, only few reports were published until now regarding the ILG deep eutectic solvent [42-49]. Leron et al. [44] showed that this DES has poor conductivity (lower than 2 mS cm^{-1} at room temperature) due to its high viscosity. The successive addition of ChCl to glycerol lowers the viscosity and increases the conductivity of the mixture (from 0.74 mS cm^{-1} for 1:4 molar ratio of ChCl-glycerol to 1.30 mS cm^{-1} for 1:2 molar ratio of ChCl-glycerol), due to more available charge carriers in an increasingly less viscous solvent.

We studied here the formation of silver nanoparticles based on the use of two-electrode cell in which the Ag^+ ions are produced either by anodic dissolution of bulk Ag metal, or by dissolution of a silver salt. To our knowledge, the choline chloride – glycerol deep eutectic solvent has not been employed as an electrolysis medium for preparing large amounts of metal nanoparticles.

EXPERIMENTAL

Chemicals and materials

Choline chloride (denoted as ChCl, 2-hydroxy-N,N,N-trimethyl–ethyl-ammonium chloride, 99%), glycerol (denoted as G, 99%), silver chloride (AgCl) and poly(N-vinyl pyrrolidone) (PVP, average molecular weight 55,000 g mol^{-1}, 99.9%) were purchased from Sigma-Aldrich. All chemicals were of analytical grade and used without further purification.

The eutectic mixture (symbolized ILG) has been prepared by mixing and heating with gentle stirring

ChCl with G in 1:2 molar ratio at a temperature in the range 80–100°C, until a homogeneous, clear liquid was formed. AgCl and PVP were then introduced to prepare the electrolytes, as shown in Table 1.

Table 1. ILG based electrolytes involved in Ag nanoparticles electrochemical synthesis.

System type	Electrolyte composition
ILG	Choline chloride : glycerol (1:2 molar ratio)
ILG-PVP	ILG + 1-5 gL^{-1} PVP
ILG-Ag	ILG + 2-10 mM AgCl
ILG-PVP-Ag	ILG + 1-5 gL^{-1} PVP + 2-10 mM AgCl

Electrochemical investigation of Ag/Ag+ couple

To get more information on the electrochemical behaviour of Ag/Ag^+ couple in the ILG based electrolytes during Ag NPs electrochemical synthesis, cyclic voltammetry measurements were carried out using a three-electrode cell with a glassy carbon (GC) disk as working electrode having a geometrical surface of 0.196 cm^2 and a Pt mesh as auxiliary electrode. All electrode potentials were measured against Ag wire immersed in DES electrolyte as quasi-reference electrode; the half-cell equilibrium reaction is due to the AgCl film formed onto Ag surface in contact with the ionic liquid with certain content in chloride ions. This Ag quasi-reference electrode has the advantage of achieving the equilibrium potential in short time. It is reproducible and maintains electrode potential within long time, making it particularly well suited for comparison [50,51]. All voltammetric studies were performed at 25°C using an Autolab PGSTAT 12 potentiostat controlled with GPES software. The applied scan rates were in the range 5-100 mVs^{-1}. Before each CV measurement, the surface of GC working electrode was cleaned to remove reductive substances by polishing with 50 μm alumina paste and washing with bidistilled water.

Electrochemical synthesis of Ag nanoparticles (Ag NPs)

The electrochemical synthesis experiments were performed under mild stirring and in an open system using a pulse reverse power supply (pe86CB 3HE, Plating Electronic GmbH, Germany). The cell has a two-electrode configuration, as illustrated in Fig. 1 and contains 300 mL ionic liquid as electrolyte.

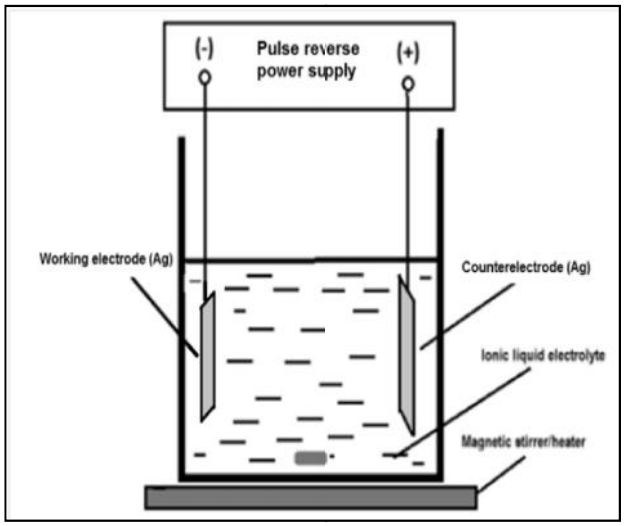

Fig. 1. Experimental set-up for Ag nanoparticles electrochemical synthesis.

Both electrodes consisted of Ag plates with 99.999% purity (30 x 20 x 0.5 mm) and exposed surface area of 6 cm^2. In other series of experiments the electrochemical synthesis was carried out involving Pt plate electrodes having the same surface area.

The electrochemical synthesis experiments have been performed at room temperature (25°C) with duration between 10-30 min. Before each experiment, the silver electrodes were hand polished by fine grade emery paper and washed with bidistilled water and a small amount of acetone and dried. Two regimes of the applied pulse reversed current have been used, as shown in Fig. 2.

After synthesis, the electrolyte containing Ag NPs was subjected to centrifugation at 4000 rpm for 15 min., with intermediary washing steps using ethanol. This sequence has been repeated for 4 times.

Characterization

The morphology and composition of the electrochemically prepared Ag NPs have been analyzed by scanning electron microscopy (SEM) associated with energy-dispersive X-ray (EDX) analysis (SU8230, HITACHI High-Technologies Corporation, Japan). Particle size distribution of the prepared Ag NPs in ILG based systems was determined by DLS (Dynamic Light Scattering) technique using a Zetasizer Nanoequipment. UV-VIS absorption spectra were recorded from 300 to 800 nm for Ag NPs dispersed in ILG medium involving a JASCO V 500 spectrophotometer.

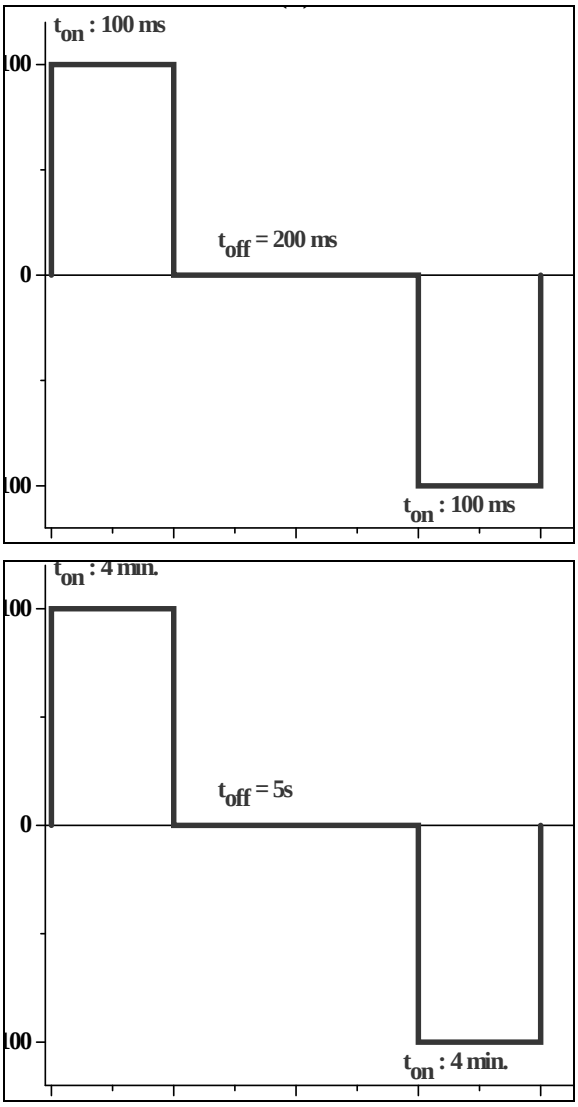

Fig. 2. Programmed electrical parameters for the pulse current electrodeposition of Ag NPs.

RESULTS AND DISCUSSION

Investigation of electrode processes by cyclic voltammetry

During the AgNPs formation there is a competition between two different cathode surface processes: (1) particles formation by electroreduction of Ag^+ ions under protection of PVP, and (2) metal deposition at the cathode surface. This second process limits the synthesis efficiency and must be minimized. We expect for PVP on the one hand to promote the nucleation of Ag NPs and on the other hand to effectively stabilize the dispersed silver nanoparticles.

Cyclic voltammetry experiments were carried out firstly in supporting electrolytes at constant temperature of 25°C (Fig. 3) to study the potential window and potentially electrochemical reactions occurring on inert glassy carbon electrode. An example of typical CV curve recorded in ILG is shown in Fig. 3a, indicating a potential window on GC electrode from about +1 V to –1 V (electrode potential *vs.* Ag quasi reference). This value of more than 2 V presents a good electrochemical stability of ILG, in agreement with CV curves recorded by Figueiredo et al. on GC, Pt and Au electrodes [42].

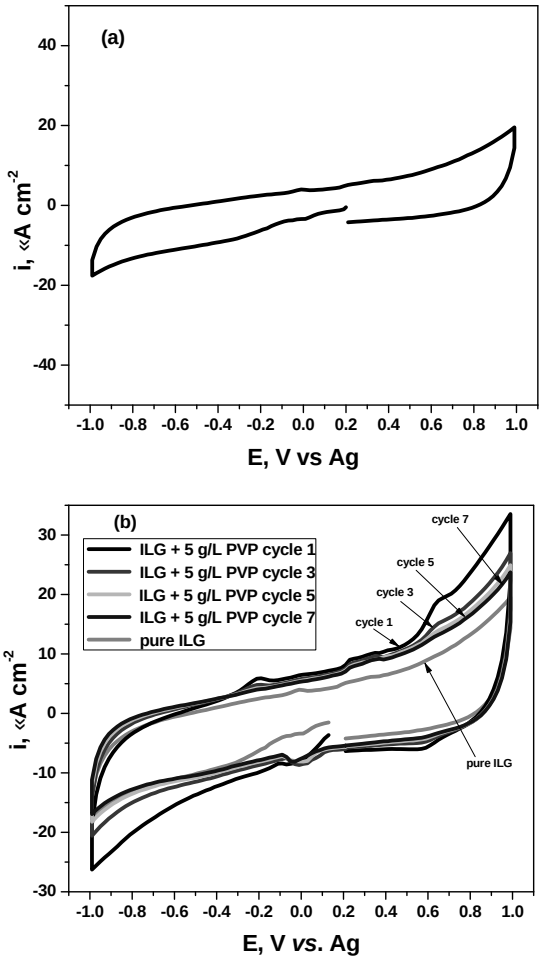

Fig. 3. CVs on GC electrode, 20 mV s^{-1} scan rate for supporting electrolytes: ILG (a); comparison of ILG with repetitive cycles of ILG + 5 gL^{-1} PVP (b).

Within this interval no peaks are observed which may suggest for the absence of processes related to any electroactive species. The increase of the cathodic current by extending the scan to negative potentials is attributed to the reduction of cholinium cation (this cation is essentially in ILG solvent), while the final increase of the anodic current is attributed to the oxidation of Cl- ions (existing also in this solvent, although they are partially complexed with glycerol) or oxidation of glycerol. Fig. 3b shows that the dissolution of PVP in ILG seems to add a small current contribution as compared to pure ILG. As a whole, the current density in ILG-PVP after 7 cycles is lower than 20 µA/cm2, very close to the pure ILG solvent. The PVP molecules, having large molecular weight, do

not allow a significant electrochemical modification.

It is worth mentioning that there is lack of information in the literature regarding Ag electrochemistry in choline chloride - glycerol based ionic liquids. Therefore, several cyclic voltammetry experiments were performed and discussed here to confirm the electrochemical reversibility of Ag/Ag^+ couple, as in the case of choline chloride – urea DES [50,51]. Fig. 4 shows CVs for ILG + AgCl (ILG-Ag) systems indicating the influence of Ag^+ concentration at constant scan rate 20 mVs^{-1} (Fig. 4a) and at various scan rates for systems with AgCl concentrations of 2, 5 and 10 mM (Figs. 4 b-d). In all the curves presented in Figure 4 a characteristic shape of the Ag^+/Ag couple voltammograms can be seen. It has a broad cathodic peak for Ag^+ reduction followed by a high limiting diffusion current and a sharp anodic peak assigned to the stripping of Ag metal from GC surface.

As shown in Fig. 4a, both cathodic and anodic peak currents increase with AgCl concentration from 5 to 16 μA, and from 23 to 54 μA, respectively. When AgCl content is higher, the cathodic peak potential shifts towards positive values (from -0.630 V to -0.470 V). The potential of the anodic peak remains constant at 0.05 V. These trends were also observed for CVs recorded at other scan rates. Moreover, the increase of the scan rate entails the increase of both cathodic and anodic peak currents for each AgCl concentration (Figs. 4 b-d). However, for ILG + 2 mM AgCl system (Fig. 4b) the shape of the cathodic curves is rather a plateau of limiting current and for the other ILG-Ag systems (with 5 and 10 mM AgCl, Figs. 4c,d) the shifting of the cathodic peak is significantly amplified with scan rate, leading to large ΔE_p differences. The high IR ohmic drop through the electrolyte due to the low electrical conductivity of ILG at room temperature could be an explanation. Therefore, we suppose that the Ag^+/Ag couple is electrochemically reversible, especially because a shift of the anodic peak potential with AgCl concentration or scan rate was not observed.

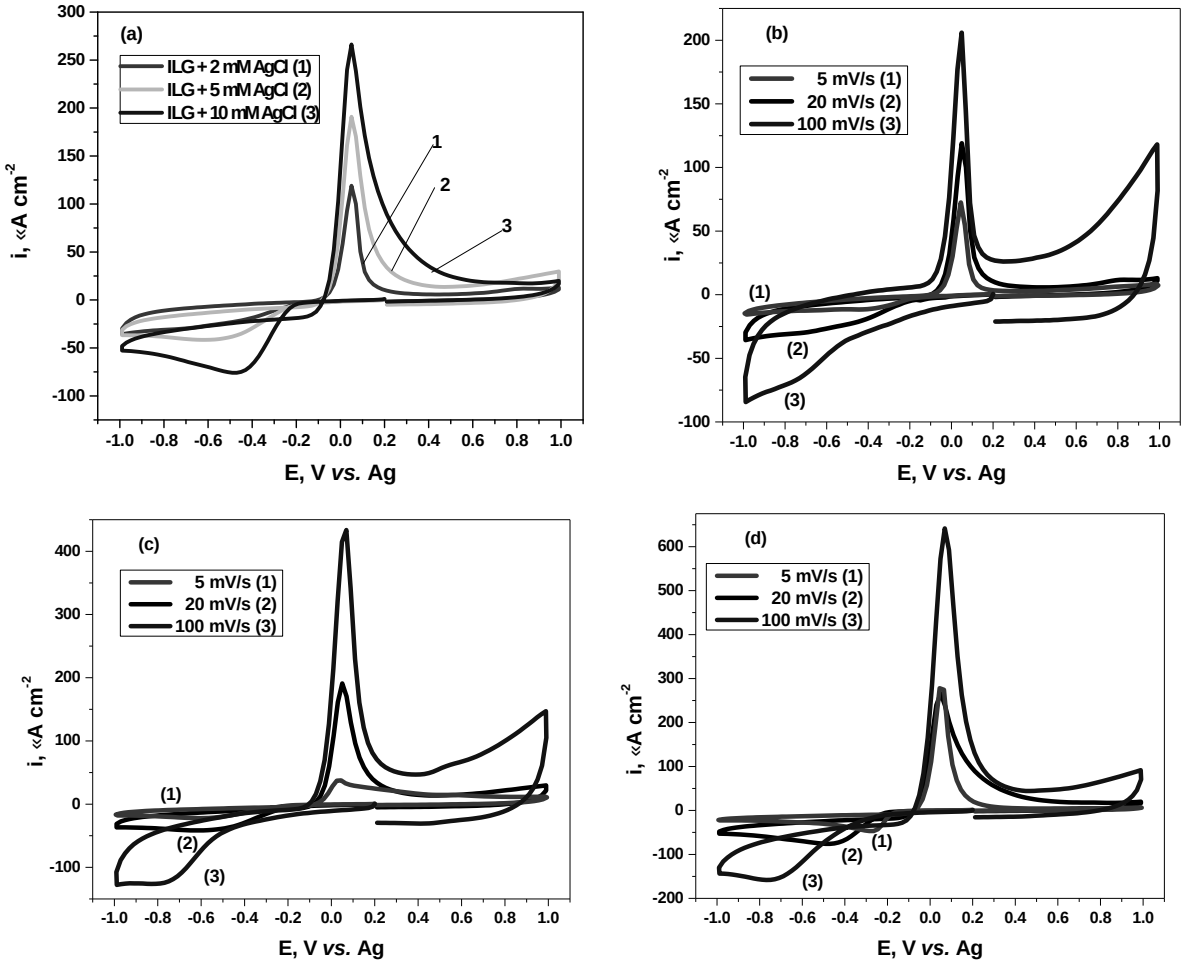

Fig. 4. CVs on GC electrode for ILG + x mM AgCl systems, showing the influence of Ag^+ concentration at constant scan rate 20 mVs^{-1} (a) and at various scan rates for 2 mM AgCl (b), 5 mM AgCl (c) and 10 mM AgCl (d).

Fig. 5 shows comparatively the families of CVs recorded during 7 repetitive cycles in ILG + 5 mM AgCl and ILG + 10 mM AgCl electrolytes. For both systems the CV curve of the first cycle is very different from the next scans, when a tendency to reach a stationary state is observed for both peak potential and peak current. The maximum value of peak currents (in both cathodic and anodic processes) is recorded in the second cycle. In addition, we suppose that supplementary waves evidenced in the first cycle may be due to the Ag nuclei formed by the underpotential deposition (UPD of Ag, at -0.015 V) and respectively to their anodic dissolution (at 0.55 V).

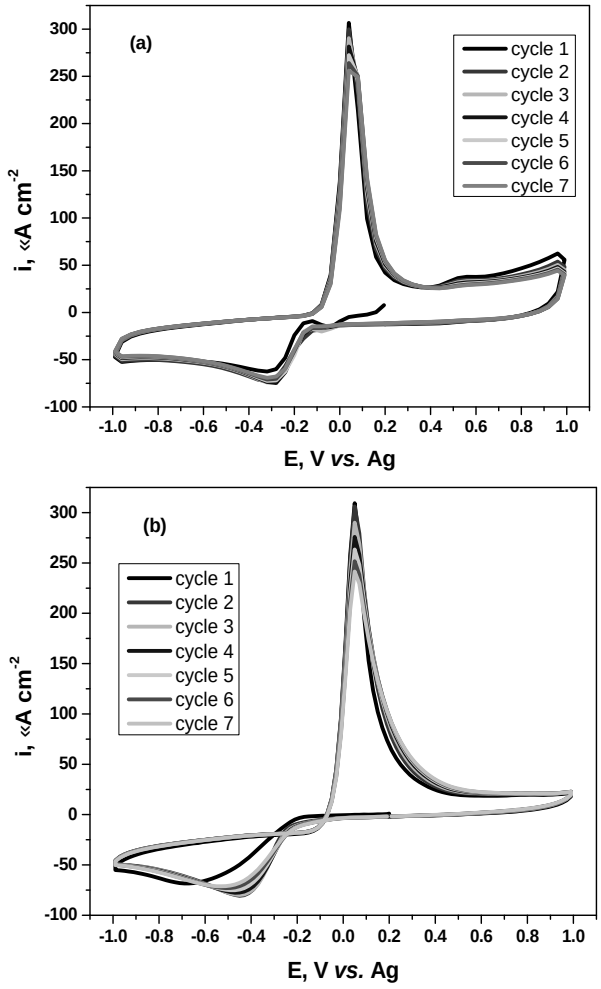

Fig. 5. Repetitive seven CV cycles on GC electrode, 20 mVs^{-1}, for ILG + 5 mM AgCl (a) and ILG + 10 mM AgCl (b).

A quantitative analysis of CVs for ILG-Ag electrolytes should take into consideration the mass-transport control (diffusion control) of a reversible cathodic process. We obtained plots (not shown here) with the cathodic peak current (I_p) almost linearly proportional to square root of the scan rate ($v^{1/2}$); the relative invariance of current function $I_p/(c \times v^{1/2})$ with Ag^+ concentration (c) allowed us to estimate the diffusion coefficient of silver ion in ILG systems, using the equation proposed by Schiffrin et al. [52,53]. Values of (0.2-1) $\times 10^{-7}$ cm^2s^{-1} at room temperature for diffusion coefficient of Ag^+ using glassy carbon electrode and choline chloride – glycerol electrolyte are much lower than usual values in aqueous electrolytes or in traditional ionic liquids (10^{-5} cm^2s^{-1}). However, they are reasonable, taking into account the high viscosity of ILG and a partial complexation of Ag^+ ions with glycerol.

Cyclic voltammetry studies for systems containing PVP as capping and stabilizer agent are very important to establish its optimum content in the electrolyte.

Fig. 6 presents an example of the recorded CV in the absence and in the presence of PVP for ILG + AgCl system at a constant scan rate. It can be observed for Ag^+ electroreduction that the cathodic peak potential shifted to more negative values whereas the peak current remains almost similar. The anodic peak corresponding to Ag dissolution as stripping appears at potentials around 0.06 V in the PVP free solution with a displacement towards 0.04 V in the presence of PVP.

The anodic peak current in the absence of PVP is significantly higher than that evidenced in the presence of PVP; this significantly decrease on PVP addition was also observed for all other ILG-PVP-Ag systems (with 0.6; 1 and 5 gL^{-1} PVP and 2, 5 and 10 mM AgCl, respectively).

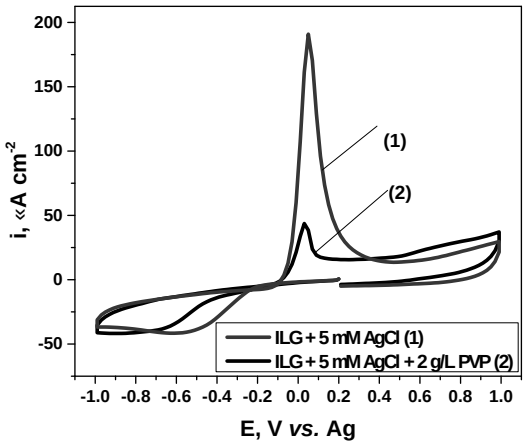

Fig. 6. Comparative CVs on GC for ILG + 5 mM AgCl system in the absence and in the presence of 2 gL^{-1} PVP (scan rate: 20 mVs^{-1}).

It can be assumed that in the PVP free solution the entire electroreduced silver has been completely dissolved anodically forming Ag^+ species, while in the PVP containing ones, just the electrodeposited silver has been again dissolved during anodic scan. In the presence of PVP, the anodic dissolution current is lower, thus suggesting that a part of

metallic silver remains into the solution as nanoparticles protected by the stabilizer. This behavior is in a good agreement with previous researches [21 and included references].

To get more information on the influence of PVP content in the electrolyte to maximize the silver nanoparticles electrosynthesis yield, cyclic voltammograms have been recorded for 7 repetitive cycles in systems with constant Ag^+ concentration and different PVP concentrations (1; 2 and 5 gL^{-1}), as exemplified in Fig. 7. For systems diluted in PVP, the evolution of the cathodic peak current with the number of cycles was not significantly influenced by PVP; this current is diminishing only at high PVP concentration (5 gL^{-1} PVP) as Figure 7a shows. The cathodic peak potential shifts to more negative values with the number of cycles.

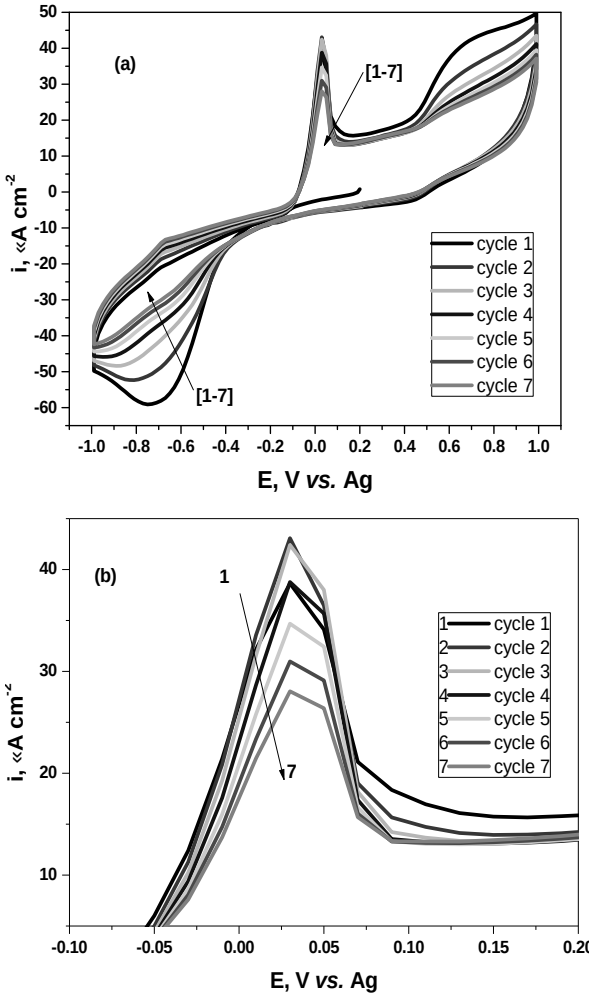

Fig. 7. Repetitive seven CV cycles on GC electrode, for ILG + 5 mM AgCl + 5 gL^{-1} PVP system (a) and details of the anodic peak for Ag stripping (b), for scan rate of 20 mVs^{-1}.

The most obvious changes are observed on the anodic branch of the voltammograms. Except for the first cycle, the anodic peak current of Ag stripping in systems with 1 and 2 gL^{-1} PVP decreases slightly with the number of cycles. However, the decrease was found to be bigger for higher PVP concentrations (of 5 gL^{-1}), although the anodic peak potential has not been shifted by cycling (Fig. 7b).

Considering the decrease of the anodic peak current as an evidence for the Ag NPs electrosynthesis rate increase, one may thus suggest that the optimum content of PVP allowing a suitable formation of Ag nanoparticles should be around 5 gL^{-1}, a slightly lower value as compared to that proposed for water based electrolytes [21].

Electrochemical synthesis of Ag NPs and characterization

Following the electrochemical synthesis process, Ag NPs of various size between 60 and 200 nm were obtained, depending on the used ILG based electrolyte, pulse reversed current regime and electrodes type. Fig. 8 comparatively presents examples of the recorded particles size distribution for Ag NPs electrosynthesized under the two regimes of the applied pulse reversed current, using Ag electrodes in the presence and in the absence of PVP. As expected, the PVP addition associated with the use of shorter pulses facilitates the decrease of the average NPs size from around 140-165 nm towards 47-63 nm. It is known that this capping agent may surround the nucleated particle restricting its further growing [34-37].

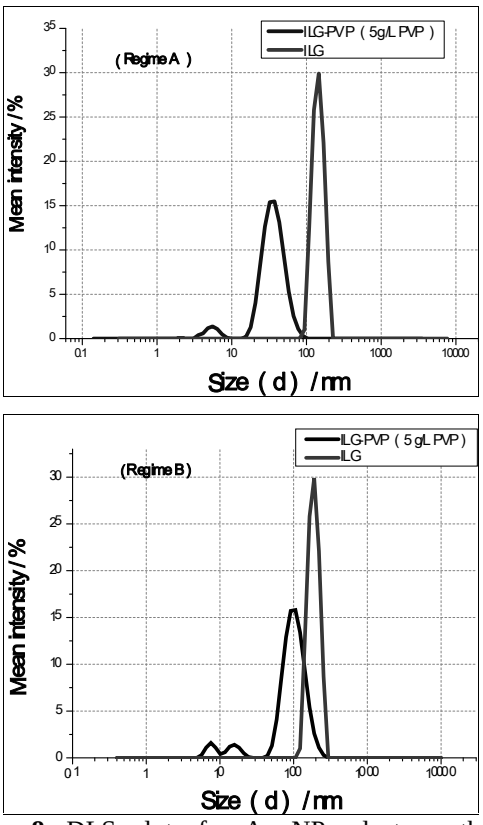

Fig. 8. DLS plots for Ag NPs electrosynthesized under regime (A) and (B) from Fig. 2 using Ag electrodes and 30 min. electrolysis time.

The particles size distribution for Ag NPs electrosynthesized under regime (B) of the applied pulse reversed current using Pt electrodes and ILG-Ag and ILG-PVP-Ag electrolytes is presented in Fig. 9. As shown, when Ag+ ions are already present in the electrolyte, the PVP addition does not act any more as a stabilizer for nanoparticles. Therefore Ag NPs of about 100-200 nm were obtained in the presence of PVP, while for ILG-Ag electrolyte their size was in the range of 70-90 nm.

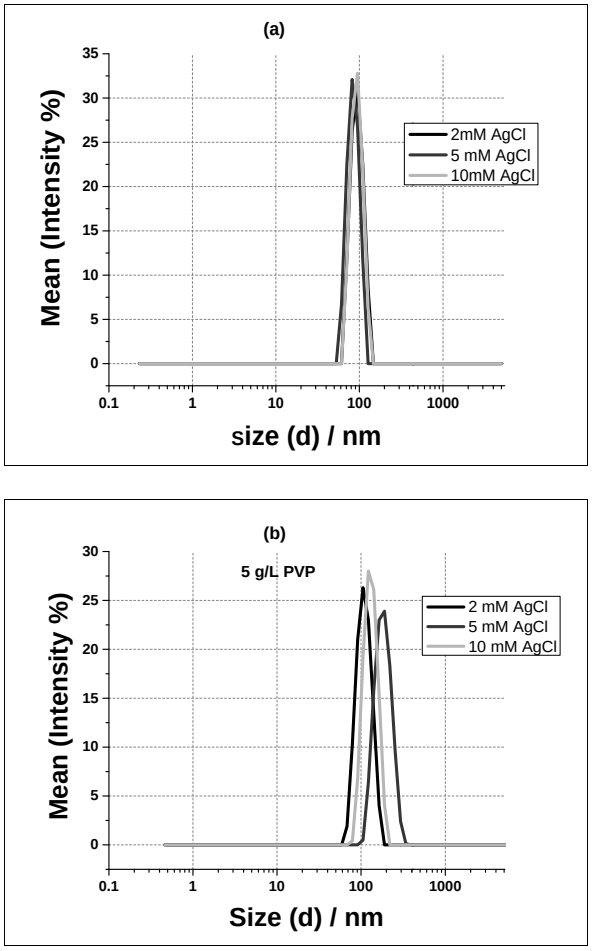

Fig. 9. DLS plots for Ag NPs electrosynthesized under regime (B), 30 min., using Pt electrodes in the absence (a) and in the presence of 5 gL^{-1} PVP (b).

In this casethe role of the ionic liquid itself, which also may act in a similar manner, should be taken into consideration. Thus, the organic cations (cholinium) of the ionic liquid may surround the Ag nuclei produced from Ag^+ electrochemical reduction during the negative pulse, in this way stabilizing the particles size and their dispersion in the ionic liquid. Quite similar behavior has been reported by Fukui et al. [29] in the case of Ag NPs preparation using BMPTFSA, BMITFSA, TMHATFSA, BMIOTf and EMITFSA ionic liquids containing Ag^+ ions.

SEM micrographs of Ag NPs electrochemically synthesized using different pulse reversed current regimes are shown in Figs. 10 and 11.

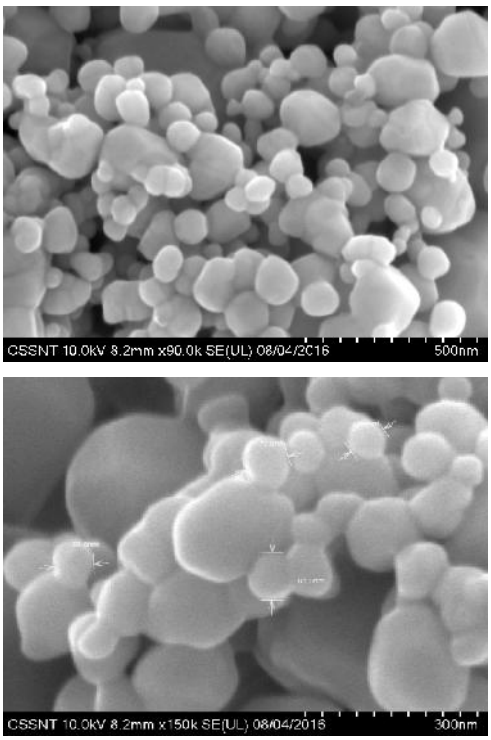

Fig. 10. SEM micrographs at different magnifications for Ag NPs electro-synthesized in ILG-PVP under regime (A) of applied pulse reversed current using Ag electrodes.

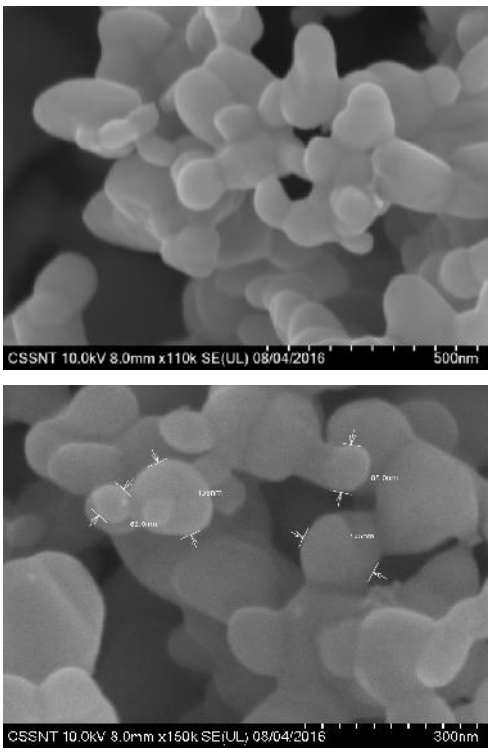

Fig. 11. SEM micrographs at different magnifications for Ag NPs electro-synthesized in ILG-PVP under regime (B) of applied pulse reversed current using Ag electrodes.

As it can be seen, the samples consist of quite spherical particles with size between 60-85 nm when regime (A) is applied, while for regime (B) larger particles of about 80-135 nm are observed.

This evidence may suggest for shorter pulses that are more appropriate to obtain smaller Ag NPs; in this way the growth step is limited, mostly facilitating the nucleation one. In addition a slight agglomeration of the nanoparticles in the SEM images may be noticed, due to their small size.

UV/VIS absorption spectra for the electrosynthesized AgNPs involving ILG have been also recorded, as exemplified in Fig. 12.

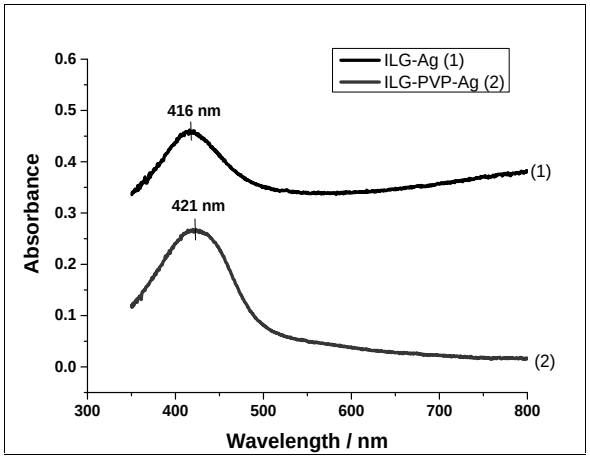

Fig. 12. UV/Vis absorption spectra of AgNPs electrosynthesized in ILG-Ag and ILG-PVP-Ag electrolytes using Pt electrodes (5 mM AgCl, 5 gL^{-1} PVP).

The absorption spectra from Fig. 12 show one distinct absorption band centered at around 416 - 420 nm, which is characteristic for the presence of metallic silver [54]. This is usually assigned to the surface plasmon excitation of silver nanoparticles with a certain distortion with respect to the spherical shape [3]. Usually, a decrease in the particle size induces a decrease in the plasmon band intensity, as it can be noticed in the case of PVP addition [55,56].

CONCLUSIONS

Based on the obtained experimental results, a novel electrochemical synthesis procedure for preparing Ag nanoparticles involving pulse reversed current and choline chloride-glycerol eutectic mixture as electrolyte, has been proposed. Voltammetric measurements showed quite reversible and diffusion controlled process of silver deposition in the electrolyte based on choline chloride –glycerol deep eutectic solvent. Through a proper selection of the applied current and of the pulse regime, the nanoparticles size may be controlled. The obtained Ag NPs showed size in the range of 60-200 nm, depending on the electrochemical synthesis conditions.

Some other important aspects such as a better understanding of the electrochemical process occurring in the choline chloride based ionic liquid electrolyte and their influence on the Ag NPs size and morphology are suggested for further investigation.

Acknowledgements: *The present work was financially supported by the Romanian Ministry of Education and Research, PNCDI II-PARTENERIATE, under research contract No.167/2012 – SELFPROPIEL and NOVTINAL-BEST project (Contract 38/2016) under M ERA Net Program.*

REFERENCES

1. A. Petica, S. Gavriliu, M. Lungu, N. Buruntea, C. Panzaru, *Mater. Sci. Eng.* B, **152(1-3)**, 22 (2008).
2. O. Akhavan, M. Abdolahad, Y. Abdi, S. Mohajerzadeh, *J. Mater. Chem.*, **21(2)**, 387 (2011).
3. L. Blandon, M. V. Vázquez, D. M. Benjumea, G. Ciro, *Portug. Electrochim. Acta*, **30(2),** 135 (2012).
4. A. Castle, E. Gracia-Espino, C. Nieto-Delgado, H. Terrones, M. Terrones, S. Hussain, *ACS Nano*, **5(4),** 2458 (2011).
5. F. Ahmadi, J. B. Raoof, R. Ojani, M. Baghayeri, M. M. Lakouraj, H. Tashakkorian, *Chinese J. Catalysis*, **36(3)**, 439 (2015).
6. C. Xie, X. Lu, K. Wang, Particle Particle Syst. Characteriz., **32(6)**, 630 (2015).
7. A. Ivanovic, S. Dimitrijevic, S. Dimitrijevic, B. Trumic, V. Marianovic, J. Petrovic, N. Vukovic, Optoelectr. Adv. Mater. Rapid Commun., **6(3-4)**, 465 (2012).
8. G. Guo, *Chinese J. Rare Metals*, **37(6)**, 922 (2013).
9. J. Tian, D. Peng, X. Wu, W. Li, H. Deng, S. Liu, *Carbohydr. Polym.*, **156**, 19 (2017).
10. S. Sahoo, S. Husale, S. Karna, S. Nayak, P. Ajayan, *J. Am. Chem. Soc.*, **133(11)**, 4005 (2011).
11. J. B. Raoof, R. Ojani, E. Hasheminejad, S. Rashid-Nadimi, *Appl. Surf. Sci.*, **258**, 2788 (2012).
12. R. Sivasubramanian, M. Sangaranarayanan, *Sensors Actuators B*, **213**, 92 (2015).
13. M. Amiri, S. Nouhi, Y. Azizian-Kalandaragh, *Mater. Chem. Phys.*, **155**, 129 (2015).
14. M. Baghayeri, M. B. Tehrani, A. Amiri, B. Maleki, S. Farhadi, *Mater. Sci. Eng. C*, **66**, 77 (2016).
15. J. Bian, Q. Li, C. Huang, Y. Guo, M. Zaw, R.-Q. Zhang, *Phys. Chem. Chem. Phys.*, **17(22)**, 14849 (2015).
16. N. Dar, K.-Y. Chen, Y.-T. Nien, I.-G. Chen, *Analyt. Lett.*, **49(8)**, 1198 (2016).
17. L. Qu, L. Dai, *J. Phys. Chem. B*, **109(29)**, 13985 (2005).
18. S. Djokić, N. Nikolić, P. Zivković, K. Popov, N. Djokić, *ECS Trans.*, **33(18)**, 7 (2011).

19. U. Mohanty, *J. Appl. Electrochem*., **41(3)**, 257 (2012).
20. K. Ignatova, *Bulgarian Chem. Commun*., **45(3)**, 357 (2013).
21. N. Dobre, A. Petica, M. Buda, L. Anicai, T. Visan, UPB Sci. Bull. Series B, **76(4)**, 127(2014).
22. C. Bosch-Navarro, J. Rourke, N. Wilson, *RSC Adv.*, **6(77)**, 73790 (2016).
23. S. Tang, X. Meng, H. Lu, S. Zhu, *Mater. Chem. Phys*., **116**, 464 (2009).
24. W. Dobbs, J.-M. Suisse, L. Douce, R. Welter, *Angew. Chem. Int. Ed.*, **45(25)**, 4179 (2006).
25. R. Bomparola, S. Caporali, A. Lavacchi, U. Bardi, *Surf. Coat. Technol*., **201(24**), 9485 (2007).
26. N. Li, X. Bai, S. Zhang, Y. Gao, L. Zheng, J. Zhang, H. Ma, *J. Dispers. Sci. Technol*., **29**,1059 (2008).
27. A. Bhatt, A. Bond, *J. Electroanal. Chem*., **619**, 1 (2008).
28. T.-H. Tsai, S. Thiagarajan, S.-M. Chen, *Electroanalysis*, **22(6),** 680 (2010).
29. R. Fukui, Y. Katayama, T. Miura, *J. Electrochem. Soc*., **158(9)**, D567 (2011).
30. B. H. R.Suryanto, C. A. Gunawan, X. Lu, C. Zhao, *Electrochim. Acta*, **81**, 98 (2012).
31. Y. Li, Q. Qiang, X. Zheng, Z. Wang, *Electrochem. Commun*., **58**, 41 (2015).
32. Y. Li, Z. Wang, C. Zhao, *J. Electrochem. Soc.*, **163(8)**, D442 (2016).
33. J. Zhu, X. Zhu, Y. Wang, *Microelectron. Eng*., **77**, 58 (2005).
34. B. Yin, H. Ma, S. Wang, S. Chen, J. *Phys. Chem. B*, **107(34)**, 8898 (2003).
35. H. Ma, B. Yin, S. Wang, Y. Jiao, W. Pan, S. Huang, S. Chen, F. Meng, *Chem. Phys. Chem*., **5(1)**, 68 (2004).
36. D. Malina, A. Sobczak-Kupiec, Z. Wzorek, Z. Kowalski, *Digest J. Nanomater. Biostruct*., **7(4)**, 1527 (2012).
37. K. M. Koczkur, S. Mourdikoudis, L. Polavarapu, S. E. Skrabalak, *Dalton Trans*. **44(41)**, 17883 (2015).
38. E. Smith, A. Abbott, K. Ryder, *Chem. Rev*., **114**, 11060 (2014).
39. A. Abo-Hamad, M. Hayyan, M. A. H. Al Saadi, M. A. Hashim, *Chem. Eng. J.*, **273**, 551 (2015).
40. G. García, S. Aparicio, R. Ullah, M. Atilhan, *Energ. Fuels*, **29**, 2616 (2015).
41. A. Abbott, R. Harris, K. Ryder, C. D'Agostino, L. Gladden, M. Mantle, *Green Chem.,* **13**, 82 (2011).
42. M. Figueiredo, C. Gomes, R. Costa, A. Martins, C. M. Pereira, F. Silva, *Electrochim. Acta*, **54**, 2630 (2009).
43. Q. Abbas, L. Binder, *ECS Trans*., **33(7)**, 49 (2010).
44. R. Leron, D. S. H. Wong, M.-H. Li, *Fluid Phase Equil*., **335**, 32 (2012).
45. Y. Y. Zhang, X. Y. Ji, X. H. Lu, *Scientia Sinica Chimica*, **44(6)**, 927 (2014).
46. A. Yadav, S. Trivedi, R. Rai, S. K. Pandey, *Fluid Phase Equil*., **367**, 135 (2014).
47. A. M. P. Sakita, R. Della Noce, C. S. Fugivara, A. V. Benedetti, *Phys. Chem. Chem. Phys.*, **18**, 25048 (2016).
48. F.S.Mjalli, O.U.Ahmed, *Korean J. Chem. Eng.*, **33(1),** 337 (2016).
49. G. H. Abdullah, M. A. Kadhom, *Int. J. Eng. Res. Develop*., **12(9)**, 73 (2016).
50. L. Anicai, A. Cojocaru, A. Florea, T. Visan, Studia Univ. Babes-Bolyai, *Chemia*, **53(1)**, 119 (2008).
51. A. Florea, A. Petica, L. Anicai, T. Visan, *UPB Sci.Bull. Series B*, **72(2)**, 115 (2010).
52. D. J. Schiffrin, *J. Electroanal. Chem*., **201,** 199 (1986).
53. L. Avaca, S. Kaufmann, K. Kontturi, L. Murtomaki, D. Schiffrin, *Berichte Bunsenges. Physik. Chemie*, 97(1), 70 (1993).
54. Z. Zhang, B. Zhao, L.Hu, *J. Solid State Chem*., **121**, 105 (1996).
55. C. Petiy, P. Lixon, M. Pileni, *J. Phys. Chem*., **97**, 12974 (1993).
56. A. Taleb, C. Petit, M. Pileni, *J. Phys. Chem. B*, **102**, 2214 (1998).

ЕЛЕКТРОХИМИЧНО ПОЛУЧАВАНЕ НА Ag НАНОЧАСТИЦИ С ПОМОЩА НА ХОЛИН ХЛОРИД - ГЛИЦЕРОЛ НАСИТЕНИ ЕВТЕКТИЧНИ РАЗТВОРИ

А. Коджару[1,2], О. Бринковеану[2], А. Г. Пантази[2], Д. Балан[2],М. Еначеску[2], Т. Висан[1,2], Л. Анисаи[2]*

[1] *Катедра по неорганична химия, физикохимия и електрохимия, Политехнически университет на Букурещ, Калеа Гривитеи 132, Букурещ*

[2] *Център за наука на повърхността и нанотехнология,Университетска Политехника на Букурещ, Сплайу Индепендентеи 313, Букурещ, Румъния*

Постъпила на 4 ноември 2016 г.; коригирана на 6 март 2017 г.

(Резюме)

В тази работа са представени резултати от изследване електрохимичния синтез на сребърни наночастици (Ag НЧи) при 25 ° C, използвайки холин хлорид - глицерол наситен евтектичен разтвор и импулсен обратим ток. Демонстрирано е, че цикличната волтаметрия е полезен инструмент за определяне на оптималното съдържание на стабилизатора поливинилпиролидон чрез анализ на стойностите на анодия пиков ток по отношение на номера на цикличната крива, като индикатор за количеството колоиден нано-Ag материал образуван в разтвора. Показано е, че двойката Ag+/Ag върху стъкловъглеродния електрод проявява почти обратимо поведение с дифузионен контрол на катодния процес и аноден стрип процес. Въз основа на измервания с Динамично светлинно разсейване и сканираща електронна микроскопия е установено, че при подходящ подбор на импулсния режим размерът на сребърните наночастици може д бъде контролиран. Получените Ag НЧи са с размери в диапазона от 60-200 нм, в зависимост от условията на електрохимичния синтез.